Exosomes Derived from Stem Cells from Apical Papilla Ameliorate Sjogren's Syndrome by Suppressing Th17 Cell Differentiation

Aochen Wang
School of Stomatology, China Medical University
Jie Liu
Centre of Science Experiment, China Medical University
Si Yu
School of Stomatology, China Medical University
Xuemei Liu
School of Stomatology, China Medical University: Zhuyi Medical University Hospital of Stomatology
Xueying Zhuang
School of Stomatology, China Medical University
Yao Liu
School of Stomatology, China Medical University
Xu Chen (chenxu@cmu.edu.cn)
Department of Paediatric Dentistry, School of Stomotology, China Medical University
https://orcid.org/0000-0002-2158-8320

Research

Keywords: stem cells from apical papilla, exosome, Sjogren's syndrome, T helper 17, PIWI-interacting RNA

Posted Date: September 8th, 2021

DOI: https://doi.org/10.21203/rs.3.rs-864685/v1

Abstract

Background: Sjogren's syndrome (SS) is a chronic autoimmune disease that is characterized by progressive lymphocyte infiltration and a decrease in the secretory function of the salivary glands. Mesenchymal stem cell (MSCs) transplantation has shown great potential in the treatment of SS. Exosomes are one of the key paracrine factors that allow MSCs to perform their functions, and are more stable and safer than MSCs. Stem cells from apical papilla (SCAP), a kind of dental stem cells that are derived from the neural crest, have a wide range of immunoregulatory properties. However, the roles of exosomes derived from SCAP (SCAP-Exo) in the treatment of SS are not clear. This study investigated the effects of SCAP-Exo on ameliorating SS and the underlying mechanisms.

Methods: SCAP-Exo were isolated and characterized by western blotting, transmission electron microscopy and nanoparticle tracking analysis. SCAP-Exo were systemically infused into SS mice *via* the tail vein. H&E staining, saliva flow rate tests, flow cytometry and enzyme-linked immunosorbent assays (ELISA) were performed to verify the therapeutic effects of SCAP-Exo. PIWI-interacting RNA (piRNA) array analysis was conducted to determine the piRNA expression profiles of SCAP-Exo, and the key pathways were analysed. A luciferase reporter assay was performed to reveal the molecular role of the exosomal hsa-piR-15254 target interleukin-6 receptor (IL-6R). Furthermore, the molecular mechanism by which hsa-piR-15254 regulated T helper 17 (Th17) cell differentiation *in vitro* was tested by flow cytometry, ELISA, and reverse transcription-quantitative polymerase chain reaction.

Results: We found that SCAP-Exo transplantation successfully improved saliva secretion, alleviated lymphocyte infiltration in the submandibular glands and reduced the proportion of Th17 cells in SS mice. Mechanistically, hsa-piR-15254 was enriched in SCAP-Exo; a luciferase reporter assay demonstrated that hsa-piR-15254 directly targeted the *IL-6R* mRNA 3’ untranslated region. Furthermore, we revealed that hsa-piR-15254 inhibited Th17 differentiation and downregulated the level of IL-17A in the supernatant and the expression levels of Th17-related genes *in vitro*.

Conclusion: This study demonstrated that SCAP-Exo had a superior therapeutic effect on SS by inhibiting Th17 cell differentiation. These data suggested that SCAP-Exo could be used in a cell-free approach for the clinical treatment of autoimmune disease.

Background

Sjogren's syndrome (SS) is a systemic autoimmune disorder that is characterized by lymphocytic infiltration of the salivary and lachrymal glands, progressively leading to dry mouth and dry eye, which severely impairs patient quality of life [1]. The pathophysiological mechanisms of SS are complex and not well characterized; they may be associated with endocrine abnormalities, immune dysfunction, and genetic and environmental factors [2]. It has been clarified that massive T cell infiltration and T cell dysfunction are at the centre of the pathogenesis of SS [3]. T cells can be categorized as T helper 1 (Th1), Th2, Th17, regulatory T cells (Tregs) or cytotoxic T cells according to their surface markers and functions

in the immune response. Among them, Th17 cells are a type of proinflammatory cell with activity mediated by interleukin 17 (IL-17), and the abnormal activation of Th17 cells promotes inflammation and induces autoimmune reactivity [4]. It has been found that the proportion of Th17 cells and the expression level of IL-17 in the peripheral blood of healthy people are extremely low and that Th17 number and IL-17 expression are significantly increased in SS patients; moreover, the expression level of IL-17 is positively correlated with the degree of lymphocyte infiltration in the salivary glands, indicating that Th17 and IL-17 play important roles in the pathogenesis of SS [5].

The current treatment options for SS are limited to pharmacological therapies, such as pilocarpine and cevimeline, which focus on stimulating saliva secretion from residual acinar cells [6]. However, almost all salivary secretory tissues have already been destroyed in most cases of SS, limiting the efficacy of this treatment [7]. Recently, with the gradual deepening of understanding of the immunoregulatory properties of mesenchymal stem cells (MSCs), a strategy based on MSCs has provided a new option for patients suffering from SS [8]. Some animal experiments have indicated that MSCs can modulate the abnormal immune status of SS mice and improve the secretory function of their salivary glands [9]. However, it is difficult for MSCs to reach the target organs through the systemic circulation, which hinders their therapeutic effect; In addition, immune rejection and the tumorigenicity of MSCs may limit their clinical applications [10]. Exosomes are extracellular macrovesicles of 30–150 nm in diameter and contain proteins, DNA, RNA, and other bioactive substances [11]. Notably, exosomes derived from MSCs (MSC-Exo) have a lower propensity to trigger immune responses and a reduced risk of allotransplantation than MSCs themselves [12]. Increasing evidence has demonstrated that MSC-Exo have immunomodulatory properties similar to those of MSCs and show efficacy against SS [13].

Stem cells from apical papilla (SCAP) are a group of neural crest-derived MSCs that can be isolated from the apical papilla of immature permanent teeth. SCAP have several advantages, including high *ex vivo* expansion capacity, abundant source material, and accessibility without iatrogenic trauma [14]. Our previous studies showed that SCAP had a strong ability to regulate T cell differentiation *in vitro* and exosomes derived from SCAP (SCAP-Exo) effectively promoted craniofacial soft tissue regeneration [15, 16]. However, whether SCAP-Exo can ameliorate SS and the underlying mechanisms need to be investigated. Noncoding RNAs (ncRNAs) are the main substances in MSC-Exo, and transmission of ncRNAs through exosomes has been proposed as a means of intercellular communication [17]. PIWI-interacting RNAs (piRNAs) are newly discovered endogenous small ncRNAs that exert their functions by binding to PIWI proteins [18]. These piRNAs were initially thought to maintain genome stability and regulate gene expression through transposon silencing, epigenetic programming, and DNA rearrangements [19]. Recent studies have indicated that piRNAs play an important role in the pathogenesis of autoimmune diseases and T cell differentiation [20, 21]. Our previous study found that piRNAs were abundantly expressed in SCAP-Exo [22], but the functions of these piRNAs have not been explored.

In this study, we explored the therapeutic potential of SCAP-Exo for the treatment of SS and the underlying mechanisms. Our findings suggested that systemic infusion of SCAP-Exo could improve the

secretory function of the salivary gland and reduce the proportion of proinflammatory cells in SS mice, which may be related to the mechanism by which SCAP-Exo suppress Th17 cell differentiation by delivering specific piRNAs. To the best of our knowledge, this was the first study demonstrating that exosomes derived from dental stem cells could be used in a cell-free approach to treat SS in the clinic.

Materials And Methods

Animals

Ten-week-old female Nod/ltj mice and ICR mice (from which the NOD/ltj strain was derived) were purchased from Liaoning Changsheng Biotechnology Co., Ltd. (Liaoning, China). Mice were maintained for 2 weeks, and 12-week-old Nod/ltj mice and ICR mice were used in this study. All animal experiment protocols were approved by the Institutional Animal Care and Use Committee of China Medical University (2020302).

Antibodies and reagents

Anti-CD9, anti-Alix, anti-calnexin, fluorescein isothiocyanate (FITC)-labelled anti-CD31, anti-CD34, anti-CD45, anti-CD90, anti-CD105, IgG isotype control, phycoerythrin (PE) -labelled anti-CD73 and IgG isotype control antibodies were purchased from Abcam (Cambridge, UK). Human FITC-labelled anti-CD4, human allophycocyanin (APC)-labelled anti-IL-17A, mouse FITC-labelled anti-CD4 and mouse PE-labelled anti-IL-17A antibodies were purchased from BD Biosciences (CA, USA). CD63 antibody and Alexa Fluor 488- and Alexa Fluor 568-conjugated secondary antibodies were purchased from Proteintech (Rosemont, IL, USA). PKH-67 kits were purchased from Sigma-Aldrich (St. Louis, MO, USA). Lipofectamine 3000 was purchased from Thermo Fisher (Eugene, Oregon, USA). The hsa-piR-15254 mimics, inhibitor and negative control were purchased from GenePharma (Suzhou, China).

SCAP isolation and identification

Ethics approval was obtained from the ethics committee of the School of Stomatology, China Medical University (202012), and written informed consent was obtained from all the participants. SCAP were collected from intact, caries-free impacted third molars with immature roots extracted from three healthy human patients (12–15 years of age) at the dental clinic of the School of Stomatology affiliated with the China Medical University. Dispase II (Boehringer Ingelheim, Mannheim, Germany) and collagenase type I (Worthington Biochemical Co., Lakewood, CO, USA) were used to digest the apical papilla. The cells were seeded in 10-cm culture dishes and cultured with alpha minimum essential medium (a-MEM; HyClone) supplemented with 15% foetal bovine serum (FBS; MRC BRL), 2 mM L-glutamine (Biosource/Invitrogen), 100 U/mL penicillin-streptomycin (HyClone), and 0.1 mM L-ascorbic acid 2-phosphate (WAKO, Japan) and maintained in a humidified atmosphere containing 5% CO_2 at 37 °C. SCAP at passage 5 were used for subsequent experiments.

Anti-human CD73 antibody labelled with PE and anti-human CD31, CD34, CD45, CD90, and CD105 (1:100; Abcam) antibodies labelled with FITC were used to detect the surface marker expression on SCAP. The expression of each surface marker was tested by flow cytometry (Becton Dickinson, Islandia, NY). The multiple differentiation potential of SCAP was evaluated by culturing the cells in adipogenic, osteogenic differentiation medium for 4 weeks and neurogenic differentiation medium for 2 weeks, followed by oil red O staining, Alizarin red S staining, and β-tubulin immunofluorescence, respectively.

SCAP-Exo isolation and identification

According to our previously published protocol, ultracentrifugation was used to separate and purify exosomes [16]. Briefly, when the 5th passage SCAP reached 80% confluence, the cells were washed three times with phosphate-buffered saline (PBS), and the supernatant was collected after 48 h of continuous culture in exosome-free serum medium (SBI, USA). The exosome purification procedure was based on differential ultracentrifugation at 4 ℃. The culture supernatants were centrifuged successively at increasing speeds: 3,000 × *g* for 20 min, 20,000 × *g* for 30 min, and 120,000 × *g* for 2 h (Beckman Optima L-100XP, USA). The isolated exosomes were resuspended in sterile PBS and stored at -80 ℃.

To verify the presence of SCAP-Exo in the isolates, transmission electron microscopy (TEM), NanoSight tracking analysis (NTA) and western blotting were performed, and SCAP-Exo identification was carried out according to the MISEV 2018 guidelines [23]. TEM (H-800, Hitachi, Japan) was performed to observe the shapes of exosomes. A NTA system (ZetaView, Germany) was employed to determine the sizes of the particles. SCAP-Exo were incubated with RIPA lysis buffer (Beyotime Biotech Co., Shanghai, China) on ice for 1 h, and their concentrations were measured by a BCA protein assay kit (Beyotime Biotech Co., Shanghai, China). The exosomes were quantified as described in our previous study. For western blotting analysis, 20 μg of each SCAP lysate or SCAP-Exo lysate sample were loaded and separated by 10% SDS-PAGE. The proteins were transferred to polyvinylidene difluoride membranes and then blotted with antibodies against Alix (1:500; Abcam), CD9 (1:500; Abcam), CD63 (1:500; Proteintech), or calnexin (1:500; Abcam). The protein bands were detected with an Odyssey CLx instrument (LI-COR, Lincoln, NE).

Transplantation of SCAP-Exo to SS mice

Female NOD/ltj mice, which suffer from dry mouth, dry eye and histopathological changes in the salivary glands and peripheral blood, are the most widely used model of SS and were used in this study; ICR mice served as a control [24]. NOD/ltj mice were injected *via* tail vein twice with 20 μg SCAP-Exo (*n* = 6) or PBS (*n* = 6), and ICR mice were injected with PBS (*n* = 6) at 12 and 14 weeks of age. At 16 weeks of age, mice were euthanized to collect spleen, peripheral blood, and submandibular gland samples.

Measurement of saliva flow rates

Mice were anaesthetized with 2.4% pentobarbital (100 μL/20 g body weight). Saliva was then collected on a cotton ball for 10 min under pilocarpine stimulation (0.2 mg/kg body weight, injected subcutaneously). The weight of the cotton ball was measured before and after saliva collection. Saliva weight was converted into saliva volume, assuming that 1 g represents 1 μL [25]. The amount of saliva was normalized to grams of body weight per 10 min.

Haematoxylin-eosin (H&E) and immunofluorescence staining

The submandibular glands were fixed in 4% buffered formaldehyde, embedded in paraffin, sectioned (5 μm thick), and stained with H&E. Inflammatory infiltrates in the submandibular glands were quantified according to the Chisholm–Mason classification criteria [26]. A portion of these submandibular glands was embedded in optimal cutting temperature compound, and 7-μm-thick sections were mounted on slides using a cryostat. To detect the infiltration of Th17 cells in the submandibular gland, frozen sections were subjected to immunofluorescence analysis for CD4 and IL-17A, which are matrix markers of Th17 cells.

Isolation of peripheral blood mononuclear cells and $CD4^+$ T lymphocytes

Human peripheral blood from three healthy donors and their peripheral blood mononuclear cells (PBMCs) were purified by Ficoll density-gradient centrifugation. Then human $CD4^+$ T lymphocytes were purified by negative selection from PBMCs using a $CD4^+$ T cell isolation kit (Miltenyi Biotec, Auburn, CA) according to the manufacturer's instructions with MACS LD (Miltenyi Biotec, Auburn, CA) and a MidiMACS magnetic separator (Miltenyi Biotec, Auburn, CA). Then, $CD4^+$ T lymphocytes (1×10^6 per well) were cultured on 24-well multiplates (Corning) in complete medium. The complete medium consisted of Dulbecco's modified Eagle's medium (DMEM, Lonza) supplemented with 10% heat-inactivated FBS, 2 mM L-glutamine, 50 mM 2-mercaptoethanol, 100 U/mL penicillin and 100 μg/ml streptomycin. Human $CD4^+$ T lymphocytes were used for the *in vitro* studies.

Th17 induction assay in SCAP-Exo co-culture

Induction of human Th17 cells was performed as previously reported [27, 28]. $CD4^+$ T lymphocytes were precultured on 24-well multiplates (1×10^6 per well) in complete medium in the presence of plate-bound anti-CD3 antibody (5 μg/mL), soluble anti-CD28 antibody (2 μg/mL), recombinant human transforming growth factor-β1 (TGF-β1) (2 ng/mL) and recombinant human IL-6 (50 ng/mL) (R&D Systems). To determine the effect of SCAP-Exo on Th17 cell differentiation *in vitro*, different concentrations of SCAP-Exo (20 μg/mL, 40 μg/mL) were added to the wells. After 3 days, floating cells

and culture medium were collected and centrifuged. The cells were subjected to flow cytometry to analyse the proportion of Th17/$CD4^+$ T cells, and the IL-17A levels in the supernatant were measured by enzyme-linked immunosorbent assay (ELISA).

Endocytosis experiments

SCAP-Exo were labelled with the PKH-67 Labelling Kit (Sigma, USA) according to the manufacturer's protocol. PKH-67-labelled exosomes were cocultured with 1×10^6 $CD4^+$ T cells in a 24-well multiplate for 6 h at 37 ℃ and 5% CO_2. Subsequently, $CD4^+$ T cells were fixed in 4% paraformaldehyde (PFA) solution, and the nuclei were stained with DAPI (Beyotime Institute of Biotechnology, China). The labelled exosomes in the $CD4^+$ T cells were imaged under a fluorescence microscope.

Bioinformatics analysis

In this experiment, we identified the most highly expressed piRNAs in SCAP-Exo and predicted their target genes by miRanda (v3.3a, www.microrna.org/microrna/home.do) and RNAhybrid (http://bibiserv.techfak.unibielefeld.de/rnahybrid). Kyoto Encyclopedia of Genes and Genomes (KEGG) pathway analysis was then performed to determine the participation of these target genes in different biological pathways and to determine the targets of piRNAs related to this study and their potential binding sites.

Firefly luciferase and Renilla luciferase assays

For the firefly luciferase and Renilla luciferase assays, 293T cells were seeded in a 96-well plate, cultured to 70% confluence, and transfected with either the IL-6R-3'UTR plasmid or hsa-piR-15254/negative control (GenePharma, China). The cells were transfected using Lipofectamine 3000 (Invitrogen, USA) and collected 48 h later. Luciferase activity in cell lysates was determined with a Dual-Luciferase Reporter Assay System (Promega, USA) according to the manufacturer's instructions. Firefly luciferase and Renilla luciferase activities were detected on a Veritas Microplate Luminometer (Promega, USA). The ratio of firefly luciferase to Renilla luciferase was calculated and normalized for each sample.

Transfection of hsa-piR-15254

$CD4^+$ T cells were seeded on 24-well multiplates (1×10^6 per well) the day before transfection. The cells were transfected with 50 nM hsa-piR-15254 mimic, 100 nM hsa-piR-15254 inhibitor, or the negative control (hsa-piR-15254-mimic-NC or hsa-piR-15254-inhibitor-NC) using Lipofectamine 3000 transfection reagent in 2 mL of α-MEM according to the manufacturer's instructions. Six hours later, the medium was removed, and the cells were washed three times with PBS and cultured with complete medium.

The transfected sequences were as follows: hsa-piR-15254 mimic (sense, 5’-UGUAGUGCGCUAUGCCGAUCGGGUGUCCCC-3’; antisense, 5’-GGACACCCAUCGGCAUACGACUAGAUU-3’), hsa-piR-15254 inhibitor (sense, 5’-GGGGACACCCAUCGGCAUACGACUAGA-3’), mimic negative control (sense, 5’-UUCUCCGAACGUGUCACGUUU-3’; antisense, 5’-AAACGUGACGUUCGGAGAA-3’), and inhibitor negative control (sense, 5’-AAACGUGACGUUCGGAGAA-3’). All oligos were synthesized by Suzhou GenePharma Gene Co. Ltd. (Suzhou, China).

Reverse transcription-quantitative polymerase chain reaction (RT-qPCR)

For gene expression analysis, cells were collected and washed three times with PBS and then lysed in RNAiso Plus (Takara, Japan). Total RNA was isolated and reverse-transcribed using the PrimeScript™ RT Reagent Kit with gDNA Eraser (Takara, Japan) to obtain cDNA. For piRNA expression analysis, after RNA isolation, first-strand cDNA was synthesized via reverse transcription using the Mqklir-X™ miRNA First Strand Synthesis Kit (Takara, Japan) according to the manufacturer’s instructions. RT-qPCR was then carried out on a Bio-Rad real-time PCR system (CFXConnect, USA) for 40 cycles with Power TB Green PCR Master Mix (Takara, Japan). The expression levels of the target genes were normalized to that of the control housekeeping gene *GAPDH*, and piRNA expression was normalized to that of U6. Gene expression data were analysed by the $2^{-\Delta\Delta Ct}$ method. The primer sequences are listed in Table 1.

Flow cytometry analysis for Th17 cell detection

Human $CD4^+$ T cells were incubated with the relevant anti-human antibodies to characterize Th17 cell subsets: FITC-CD4 and APC-IL-17A. To characterize mice Th17 cells, peripheral blood was collected from the orbital vein, and PBMCs was separated using erythrocyte lysis. Moreover, we isolated splenic PBMCs from mice. A single-cell suspension was collected by mincing mice spleen tissues through a 70 μm strainer, followed by erythrocyte lysis. Then, PBMCs from the spleen and peripheral blood were stained with FITC-CD4 and PE-IL-17A anti-mouse antibodies to identify Th17 cells. The stained cells were assayed by flow cytometry (Becton Dickinson, Islandia, NY), and the data were analysed with FlowJo software (FlowJo LLC, version 10.6.0).

IL-17A ELISA

Culture supernatant was collected from the coculture of SCAP-Exo with activated $CD4^+$ T cells. Blood serum was obtained from peripheral blood collected from NOD/ltj and ICR mice. All samples were stored at -80 ℃ until use and recentrifuged before ELISA. The expression levels of IL-17A were measured according to the manufacturer's protocols for the human and mouse IL-17A enzyme-linked immunosorbent assay kits (BD Biosciences).

Statistical analysis

Three biological replicates were performed for all procedures to verify the results. The data were recorded as the mean ± standard deviation (SD). Comparisons between two groups were analysed using an independent two-tailed Student's *t* test, and comparisons among more than two groups were performed using one-way analysis of variance (ANOVA) with SPSS 20.0 software (SPSS Inc., Chicago, IL, USA). A value of $P < 0.05$ was considered to indicate statistical significance.

Results

Characterization of SCAP and identification of SCAP-Exo

SCAP showed a characteristic spindle-like morphology under a microscope (Fig. 1a). Subsequently, Alizarin red S staining and oil red O staining showed that SCAP formed mineralized matrix and oil droplets under osteogenic and adipogenic induction conditions, respectively (Fig. 1b-c). When SCAP were cultured in neurogenic induction medium for 2 weeks, immunostaining showed that the cells expressed the neurogenic marker β-tubulin (Fig. 1d). In addition, we used flow cytometry analysis to demonstrate that SCAP were positive for the mesenchymal markers CD73, CD90, and CD105 but did not express the haematopoietic lineage markers CD31, CD34, and CD45 (Fig. 1e).

TEM indicated that the vesicles were round cup-shaped structures (Fig. 1f). Using the NTA technique, we observed that the diameter distribution of these particles ranged from 30 to 150 nm with a mean of 113 nm (Fig. 1g). Western blotting analysis showed that SCAP-Exo expressed exosome-specific antibodies against CD9, CD63, and Alix but did not express the endoplasmic reticulum-specific protein calnexin (Fig. 1h).

SCAP-Exo transplantation ameliorated SS symptoms by downregulating Th17

Female NOD/ltj mice began to show submandibular gland lymphocyte infiltration at 8 weeks of age. Infiltration became obvious at 12 weeks of age, at the same time the mice showed symptoms of decreased salivary gland secretion [24]. To determine whether SCAP-Exo transplantation has therapeutic effects in SS, we injected SCAP-Exo into NOD/ltj mice *via* the tail vein twice, at 12 and 14 weeks of age, and then collected samples at 16 weeks of age. H&E staining showed that there was almost no lymphocyte infiltration in the submandibular glands of healthy ICR mice. In contrast, obvious masses of infiltrating lymphocytes were observed in the submandibular glands of NOD/ltj mice, and the level of saliva secretion of NOD/ltj mice was significantly lower than that of ICR mice, in accordance with the symptoms of SS, which indicated that the NOD/ltj mice used in this experiment were an appropriate animal model. In NOD/ltj mice treated with SCAP-Exo, the saliva secretion level was significantly improved, and the mass of infiltrating lymphocytes in the submandibular gland was decreased and even

disappeared (Fig. 2a-c). These results indicated that SCAP-Exo had a significant therapeutic effect, ameliorating SS symptoms.

Flow cytometry analysis and ELISA showed that the proportion of Th17/$CD4^+$ T cells in the peripheral blood and spleen and the expression level of IL-17A in the serum of NOD/ltj mice were significantly higher than those in ICR mice, but the proportion of Th17/$CD4^+$ T cells and the expression level of IL-17A were significantly downregulated after SCAP-Exo transplantation (Fig. 2d-h). Furthermore, we examined the level of Th17 infiltration in the submandibular glands. Immunofluorescence staining revealed that CD4 and IL-17A double-positive Th17 cells infiltrated the submandibular glands of NOD/ltj mice, while the number of Th17 cells was significantly decreased after SCAP-Exo treatment (Fig. 2i). These data suggested that SCAP-Exo had an obvious inhibitory effect on Th17 and IL-17A levels in NOD/ltj mice.

SCAP-Exo inhibited the differentiation of $CD4^+$ T cells to Th17 cells *in vitro*

$CD4^+$ T cells were isolated from healthy human peripheral blood by immunomagnetic beads. Microscopy indicated that the $CD4^+$ T cells were round and suspended in the culture medium (Fig. 3a), and the purity of $CD4^+$ T cells as detected by flow cytometry was more than 90% (Fig. 3b). Subsequently, we incubated freshly isolated $CD4^+$ T cells with SCAP-Exo labelled with PKH-67 green fluorescent membrane linker dye for 6 h. Fluorescence microscopy showed that PKH-67-labelled SCAP-Exo surrounded the nuclei of $CD4^+$ T cells (Fig. 3c), indicating that SCAP-Exo could be endocytosed by $CD4^+$ T cells and had the potential to deliver their contents to $CD4^+$ T cells. Furthermore, TGF-β1 and IL-6 have been shown to be critical for Th17 cell differentiation both *in vitro* and *in vivo* [27]. To further verify the immunomodulatory capacity of SCAP-Exo, we added different amounts of SCAP-Exo to the $CD4^+$ T cells to Th17 cells induction system. Flow cytometry analysis and ELISA suggested that the proportion of Th17/$CD4^+$ T cells and the IL-17A level in the supernatant were markedly decreased after adding 20 μg/mL SCAP-Exo or 40 μg/mL SCAP-Exo to the induction system, and the inhibitory effects of 40 μg/mL SCAP-Exo were more pronounced (Fig. 3d-f). Th17 cells are characterized by the expression of IL-17A, IL-21 and the lineage-defining transcription factor retinoic acid receptor-related orphan receptors γt (RORγt), and the mRNA expression levels of these three genes are positively correlated with Th17 cell differentiation [29]. RT-qPCR revealed that SCAP-Exo could significantly inhibit the mRNA expression levels of *IL-17A*, *IL-21* and *RORγt* in $CD4^+$ T cells, and the effect of 40 μg/mL SCAP-Exo was more obvious (Fig. 3g). These data suggested that SCAP-Exo inhibit the differentiation of $CD4^+$ T cells to Th17 cells.

IL-6R mRNA is a direct target of hsa-piR-15254

Since piRNAs play an important role in T cell differentiation, piRNAs array analysis was conducted to determine the piRNA expression profiles of SCAP-Exo. We performed KEGG pathway analysis on the

target genes of the top 40 piRNAs expressed in SCAP-Exo. Functional enrichment analysis revealed that the genes in the network were significantly involved in the Th17 cell differentiation signalling pathway (Fig. 4a), which was consistent with the finding that SCAP-Exo inhibited the differentiation of $CD4^+$ T cells to Th17 cells. These data indicated that piRNAs might play a role in the regulation of Th17 cell differentiation by SCAP-Exo.

Furthermore, we examined the piRNAs related to the Th17 cell differentiation signalling pathway, sequencing and RT-qPCR showed that the expression level of hsa-piR-15254 was much higher than that of other piRNAs (hsa-piR-6426, hsa-piR-5660) (Fig. S1). The target gene prediction results found that hsa-piR-15254 may target the mRNA of IL-6R, which is the key signal of Th17 cell differentiation [30]. Luciferase reporter assay results confirmed that hsa-piR-15254 overexpression decreased the luciferase activity in the wild-type group ($P < 0.001$) and did not affect the activity in the mutant group ($P < 0.001$; Fig. 4b-c). RT-qPCR revealed that after coculture with SCAP-Exo, the expression of hsa-piR-15254 in $CD4^+$ T cells was significantly increased, indicating that SCAP-Exo could upregulate the expression level of hsa-piR-15254 in $CD4^+$ T cells (Fig. 4d). Then, we applied mimics and an inhibitor of hsa-piR-15254 to overexpress or downregulate the expression level of hsa-piR-15254 in $CD4^+$ T cells (Fig. 4e-f). We found that the mRNA level of *IL-6R* was diminished in SCAP-Exo-treated $CD4^+$ T cells and hsa-piR-15254-overexpressing $CD4^+$ T cells but upregulated in the hsa-piR-15254 inhibitor group (Fig. 4g). These experimental data further illustrated the inhibitory effect of hsa-piR-15254 on *IL-6R* mRNA expression.

SCAP-Exo inhibited the differentiation of $CD4^+$ T cells to Th17 cells *via* hsa-piR-15254

To determine whether exosomal hsa-piR-15254 from SCAP inhibited the differentiation of $CD4^+$ T cells to Th17 cells, hsa-piR-15254 was either overexpressed or downregulated in Th17 induction medium. Flow cytometry analysis suggested that the proportion of Th17/$CD4^+$ T cells was significantly decreased in the hsa-piR-15254-overexpressing group, and the effect of hsa-piR-15254-overexpression was similar to that of SCAP-Exo administration. However, when the hsa-piR-15254 inhibitor was added to the SCAP-Exo treatment group, the proportion of Th17/$CD4^+$ T cells increased significantly (Fig. 5a-b). In addition, the concentration of IL-17A in the supernatant and the mRNA expression levels of Th17-related genes were detected by ELISA and RT-qPCR. We found that hsa-piR-15254 mimics suppressed the concentration of IL-17A in the supernatant and the mRNA expression of *IL-17A*, *IL-21* and *RORγt* in $CD4^+$ T cells, while the hsa-piR-15254 inhibitor exerted the opposite effects (Fig. 5c-d). Therefore, these data indicated that SCAP-Exo inhibited the differentiation of $CD4^+$ T cells to Th17 cells *via* hsa-piR-15254.

Discussion

The current therapies for SS are based mainly upon corticosteroids and immune suppressants, which only alleviate minor symptoms, and long-term treatment can lead to severe adverse effects [31]. Therefore, the identification of a therapeutic approach for SS with high efficiency and few side effects has been a research focus. Tissue-derived allogeneic MSCs, including those from bone marrow and umbilical cord, alleviate experimental and clinical SS, but variability among donors and limited sources of these tissue-derived MSCs hinder their application [32]. SCAP are a type of dental stem cell that has the advantages of fewer ethical concerns, a readily accessible source, and easy and minimally invasive collection [14]. In addition, our previous studies have found that SCAP can regulate T cell differentiation by paracrine action [15]. Exosomes, which contain compound bioactive compounds, are the key factors in MSC paracrine action. Compared to MSCs, MSC-Exo are much safer and more feasible for clinical applications due to their superior stability and related lower costs of storage, transport, and recovery [33, 34]. MSC-Exo have shown immunomodulatory effects similar to those of MSCs. However, there has been no report on the therapeutic effect of SCAP-Exo on SS.

Nod/ltj mice are the most commonly used animal model of SS, beginning to show hypofunction of salivary glands and continued lymphocyte infiltration at 8–12 weeks of age [24]. Our study also confirmed that lymphocyte infiltration and secretory dysfunction in the salivary glands were decreased at 12–16 weeks of age. In 16-week-old mice, we found that the saliva flow rate of NOD/ltj mice injected with SCAP-Exo was significantly improved compared with that of NOD/ltj mice injected with PBS. H&E staining showed that the mass of infiltrating lymphocytes in the submandibular gland of the NOD/ltj mice treated with SCAP-Exo were significantly reduced, with only scattered lymphocyte cell infiltration. The Chisholm *&* Mason histopathology grades ranged from Grade □ to □, similar to the results previously reported for MSC therapy [32, 35].

The infiltrating lymphocytes in the salivary glands of SS are mainly $CD4^+$ T cells [36]. Recently, it has been reported that Th17 cells play a particularly important role in the pathogenesis and development of SS and that infiltrated lymphocyte-derived IL-17 can impair the tight junction barrier of glandular epithelial cells to alter the secretory function of the submandibular gland in SS patients and mice [37, 38]. An animal experiment revealed that the salivary glands of IL-17A-knockout SS mice did not show obvious lymphocyte infiltration and dysfunction, whereas when the function of Th17 cells was restored, the salivary secretion level was reduced rapidly [39]. Therefore, therapeutics targeting Th17 and IL-17A should be highly effective against SS. In this experiment, SCAP-Exo showed a significant downregulating effect on the level of Th17 cells in the peripheral blood, spleen, and submandibular glands of NOD/ltj mice, and the expression level of IL-17A in the serum also decreased. These evidences indicate that systemic infusion of SCAP-Exo may play a therapeutic role by inhibiting the differentiation of Th17 cells in SS mice, but the effect of SCAP-Exo on the differentiation of Th17 cells needs to be further confirmed. Thus, we extracted $CD4^+$ T cells from peripheral blood, constructed a Th17 cell differentiation induction system to simulate the imbalance of Th17/$CD4^+$ T cell proportions in SS patients. Then, we found that SCAP-Exo effectively inhibited the differentiation of $CD4^+$ T cells to Th17 cells and effectively downregulated the expression of IL-17A in the supernatant. SCAP-Exo also exerted inhibitory effects on

the mRNA expression levels of *IL-17A*, *IL-21* and *RORγt*, suggesting that SCAP-Exo were involved in regulating the expression of genes in the Th17 cell differentiation signalling pathway.

The biological functions of MSC-Exo are related to their abundance of MSC-specific bioactive molecules, including lipids, proteins, microRNAs, and ncRNAs [40, 41]. NcRNAs are an important component of MSC-Exo. Many studies suggest that MSC-Exo can regulate the biological functions and gene expression of recipient cells by delivering ncRNAs. piRNAs are a new type of small ncRNA discovered in 2006 and are the most abundant type of ncRNA [42]. Like microRNAs, piRNAs form an RNA-inducing silencing complex with argonaut family proteins, bind the 3' untranslated regions (3'UTRs) of target mRNAs, and then mediate the degradation of the targeted mRNA or inhibit its translation [43, 44]. Recent research has found that piRNAs are differentially expressed in synovial fibroblasts of rheumatoid arthritis patients compared with controls and are also involved in the release of inflammatory cytokines [20]. Zhong *et al*. also found that piRNAs inhibited Th2 differentiation by downregulating *IL-4* mRNA expression in human $CD4^+$ T cells [21]. These findings indicate that piRNAs have the potential to exert immunomodulatory effects by regulating T cells. Therefore, we speculated that the function of SCAP-Exo in inhibiting Th17 cell differentiation may be related to piRNAs.

Furthermore, we conducted a bioinformatics analysis on the target genes of the most highly expressed piRNAs in SCAP-Exo. KEGG pathway analysis showed that the target genes of the highly expressed piRNAs (hsa-piR-15254, hsa-piR-5660 and hsa-piR-6426) in SCAP-Exo were enriched in the Th17 cell differentiation signalling pathway. Among them, the expression level of hsa-piR-15254 was much higher than that of other piRNAs, and the luciferase reporter assay results further confirmed that *IL-6R* mRNA is a direct target of hsa-piR-15254. IL-6R is an important surface receptor on $CD4^+$ T cells, and the binding of extracellular IL-6 by TGF-β preferentially induces the differentiation of $CD4^+$ T cells into Th17 cells, whereas the function of IL-6 at the cell surface requires binding to IL-6R [45]. Several studies suggest that ncRNAs can inhibit the differentiation of $CD4^+$ T cells into Th17 cells by inhibiting the expression of *IL-6R* mRNA [46, 47]. Therefore, we inferred that SCAP-Exo degraded *IL-6R* mRNA by delivering its highly expressed hsa-piR-15254 to $CD4^+$ T cells, thereby inhibiting the differentiation of Th17 cells. To further test this hypothesis, we employed hsa-piR-15254 mimics and inhibitors to overexpress or downregulate hsa-piR-15254 levels, respectively, in a Th17 induction system to investigate the biological function of hsa-piR-15254. We found that overexpression of hsa-piR-15254 inhibited Th17 cell differentiation, while downregulation of hsa-piR-15254 increased the proportion of Th17/$CD4^+$ T cells. Moreover, RT-qPCR results confirmed that the mRNA expression levels of *IL-6R* had a negative relationship with the expression levels of hsa-piR-15254, and overexpression of hsa-piR-15254 also downregulated the mRNA expression levels of the Th17-related genes *IL-17A*, *IL-21* and *RORγt*. These data strongly indicated that the inflammation-suppressive function of SCAP-Exo was mediated by hsa-piR-15254. These findings may have major implications for the treatment of SS by targeting Th17 cells.

Therein, we reported for the first time that exosomes derived from dental stem cells had a certain therapeutic effect on the secretory function and inflammatory cell infiltration of salivary glands in SS

mice and found that they downregulated the expression of Th17 cells in the peripheral blood, spleen, and submandibular glands. Moreover, we demonstrated that SCAP-Exo bearing hsa-piR-15254 inhibited the differentiation of $CD4^+$ T cells to Th17 cells *in vitro.* However, further *in vivo* experiments are needed to verify the function of hsa-piR-15254. Additionally, other ncRNAs and proteins in SCAP-Exo may also play a role in the treatment of SS. Research on the functions of these active substances will clarify the therapeutic mechanism of SCAP-Exo.

Conclusion

In summary, this study revealed that systematic SCAP-Exo transplantation exerted superior therapeutic effects in SS mice, improving the secretory function of the salivary glands and downregulating inflammatory cells. We also demonstrated the inhibitory effects of SCAP-Exo on Th17 cell differentiation, which was related to the degradation of *IL-6R* mRNA mediated by hsa-piR-15254. These findings suggest that SCAP-Exo can regulate the immunological status and provide a new strategy involving SCAP-Exo as a cell-free approach to treat SS in the clinic.

Abbreviations

SS: Sjogren's syndrome; Th17: T helper 17; SCAP: stem cells from apical papilla; SCAP-Exo: exosomes derived from stem cells from apical papilla; piRNAs: PIWI-interacting RNAs; IL-6R: interleukin 6 receptor; IL-17A: interleukin 17; IL-21: interleukin 21; RORγt: retinoic acid receptor-related orphan receptors γt; MSCs: mesenchymal stem cells; MSC-Exo: exosomes derived from mesenchymal stem cells; ncRNAs: non-coding RNAs; PE: phycoerythrin; FITC: fluoresceine isothiocyanate; PBS: phosphate-buffered saline; TEM: transmission electron microscopy; NTA: NanoSight tracking analysis; PBMCs: peripheral blood mononuclear cells; TGF-β1: transforming growth factor-β1; ELISA: enzyme-linked immunosorbent assay; PFA: paraformaldehyde; KEGG: Kyoto Encyclopedia of Genes and Genomes; RT-qPCR: reverse transcription-quantitative polymerase chain reaction; SD: standard deviation; ANOVA: one-way analysis of variance; H&E: haematoxylin and eosin

Declarations

Ethics approval and consent to participate:

This research was conducted according to the Institutional Animal Care and Use Committee of China Medical University (2020302).

Consent for publication:

Not applicable.

Competing interests:

The authors declare that they have no competing interests.

Acknowledgements:

Not applicable.

Authors’ contributions:

ACW: Conception and design, data collection, data analysis and interpretation, manuscript writing, final approval of manuscript. JL: Data analysis and interpretation. SY: Data collection, provision of study material. XML: Data collection, provision of study material. XYZ: Data collection, provision of study material. YL: Data analysis and interpretation, manuscript writing, final approval of manuscript. XC: Conception and design, financial support, data analysis and interpretation, final approval of manuscript. All authors read and approved the final manuscript.

Funding:

This work was supported by grants from the National Natural Science Foundation of China (82071100 to X.C.), and the Department of Science and Technology of Liaoning Province (2018225061 to X.C.).

Availability of data and materials:

The data used to support the findings of this study are available from the corresponding author upon reasonable request.

References

1. Mariette X, Criswell LA. Primary Sjögren's syndrome. N Engl J Med. 2018;378:931–9.
2. Abughanam G, Elkashty OA, Liu Y, Bakkar MO, Tran SD. Mesenchymal stem cells extract (mscse)-based therapy alleviates xerostomia and keratoconjunctivitis sicca in Sjogren's syndrome-like disease. Int J Mol Sci. 2019;20:4750.
3. Yao Y, Ma JF, Chang C, Xu T, Gao CY, Gershwin ME, Lian ZX. Immunobiology of T cells in Sjögren's syndrome. Clin Rev Allergy Immunol. 2021;60:111–31.
4. Yasuda K, Takeuchi Y, Hirota K. The pathogenicity of Th17 cells in autoimmune diseases. Semin Immunopathol. 2019;41:283–97.

5. Alunno A, Carubbi F, Bartoloni E, Bistoni O, Caterbi S, Cipriani P, Giacomelli R, Gerli R. Unmasking the pathogenic role of IL-17 axis in primary Sjögren's syndrome: a new era for therapeutic targeting? Autoimmun Rev. 2014;13:1167–73.
6. Stefanski AL, Tomiak C, Pleyer U, Dietrich T, Burmester GR, Dörner T. The diagnosis and treatment of Sjögren's syndrome. Dtsch Arztebl Int. 2017;114:354–61.
7. Błochowiak K, Celichowski P, Kempisty B, Iwanik K, Nowicki M. Transcriptomic profile of genes encoding proteins involved in pathogenesis of Sjögren's syndrome related xerostomia-molecular and clinical trial. J Clin Med. 2020;9:3299.
8. Gao F, Chiu SM, Motan DA, Zhang Z, Chen L, Ji HL, Tse HF, Fu QL, Lian Q. Mesenchymal stem cells and immunomodulation: current status and future prospects. Cell Death Dis. 2016;7:e2062.
9. Du ZH, Ding C, Zhang Q, Zhang Y, Ge XY, Li SL, Yu GY. Stem cells†from exfoliated†deciduous†teeth alleviate hyposalivation caused by Sjögren syndrome. Oral Dis. 2019;25:1530–44.
10. Jeong JO, Han JW, Kim JM, Cho HJ, Park C, Lee N, Kim DW, Yoon YS. Malignant tumor formation after transplantation of short-term cultured bone marrow mesenchymal stem cells in experimental myocardial infarction and diabetic neuropathy. Circ Res. 2011;108:1340–7.
11. Yang D, Zhang W, Zhang H, Zhang F, Chen L, Ma L, et al. Progress, opportunity, and perspective on exosome isolation-efforts for efficient exosome-based theranostics. Theranostics. 2020;10:3684–707.
12. Tao H, Chen X, Cao H, Zheng L, Li Q, Zhang K, et al. Mesenchymal stem cell-derived extracellular vesicles for corneal wound repair. *Stem Cells Int*. 2019; 2019: 5738510.
13. Hai B, Shigemoto-Kuroda T, Zhao Q, Lee RH, Liu F. Inhibitory effects of ipsc-mscs and their extracellular vesicles on the onset of sialadenitis in a mouse model of Sjögren's syndrome. *Stem Cells Int*. 2018; 2018: 2092315.
14. Sonoyama W, Liu Y, Fang D, Yamaza T, Seo BM, Zhang C, et al. Mesenchymal stem cell-mediated functional tooth regeneration in swine. PloS One. 2006;1:e79.
15. Liu XM, Liu Y, Yu S, Jiang LM, Song B, Chen X. Potential immunomodulatory effects of stem cells from the apical papilla on Treg conversion in tissue regeneration for regenerative endodontic treatment. Int Endod J. 2019;52:1758–67.
16. Liu Y, Zhuang X, Yu S, Yang N, Zeng J, Liu X, Chen X. Exosomes derived from stem cells from apical papilla promote craniofacial soft tissue regeneration by enhancing Cdc42-mediated vascularization. Stem Cell Res Ther. 2021;12:76.
17. Ti D, Hao H, Fu X, Han W. Mesenchymal stem cells-derived exosomal microRNAs contribute to wound inflammation. Sci China Life Sci. 2016;59:1305–12.
18. Aravin A, Gaidatzis D, Pfeffer S, Lagos-Quintana M, Landgraf P, Iovino N, et al. A novel class of small RNAs bind to MILI protein in mouse testes. Nature. 2006;442:203–7.
19. Rojas-Ríos P, Simonelig M. piRNAs and PIWI proteins: regulators of gene expression in development and stem cells. Development. 2018;145:dev161786.

20. Pleštilová L, Neidhart M, Russo G, Frank-Bertoncelj M, Ospelt C, Ciurea A, et al. Expression and regulation of PIWIL-proteins and PIWI-interacting RNAs in rheumatoid arthritis. PLoS One. 2016;11:e0166920.
21. Zhong F, Zhou N, Wu K, Guo Y, Tan W, Zhang H, et al. A SnoRNA-derived piRNA interacts with human interleukin-4 pre-mRNA and induces its decay in nuclear exosomes. Nucleic Acids Res. 2015;43:10474–91.
22. Wang A, Liu J, Zhuang X, Yu S, Zhu S, Liu Y, Chen X. Identification and comparison of piRNA expression profiles of exosomes derived from human stem cells from the apical papilla and bone marrow mesenchymal stem cells. Stem Cells Dev. 2020;29:511–20.
23. Théry C, Witwer KW, Aikawa E, Alcaraz MJ, Anderson JD, Andriantsitohaina R, et al. Minimal information for studies of extracellular vesicles 2018 (MISEV2018): A position statement of the international society for extracellular vesicles and update of the MISEV2014 guidelines. J Extracell Vesicles. 2018;7:1535750.
24. Yamano S, Atkinson JC, Baum BJ, Fox PC. Salivary gland cytokine expression in NOD and normal BALB/c mice. Clin Immunol. 1999;92:265–75.
25. Soyfoo MS, Bolaky N, Depoortere I, Delporte C. Relationship between aquaporin-5 expression and saliva flow in streptozotocin-induced diabetic mice. Oral Dis. 2012;18:501–5.
26. Chisholm DM, Mason DK. Labial salivary gland biopsy in Sjögren's disease. J Clin Pathol. 1968;21:656–60.
27. Yamaza T, Kentaro A, Chen C, Liu Y, Shi Y, Gronthos S, Wang S, Shi S. Immunomodulatory properties of stem cells from human exfoliated deciduous teeth. Stem Cell Res Ther. 2010;1:5.
28. Yang R, Yu T, Liu D, Shi S, Zhou Y. Hydrogen sulfide promotes immunomodulation of gingiva-derived mesenchymal stem cells via the Fas/FasL coupling pathway. Stem Cell Res Ther. 2018;9:62.
29. Leppkes M, Becker C, Ivanov II, Hirth S, Wirtz S, Neufert C, et al. RORgamma-expressing Th17 cells induce murine chronic intestinal inflammation via redundant effects of IL-17A and IL-17F. Gastroenterology. 2009;136:257–67.
30. Chen X, Zhang M, Liao M, Graner MW, Wu C, Yang Q, Liu H, Zhou B. Reduced Th17 response in patients with tuberculosis correlates with IL-6R expression on CD4 + T Cells. Am J Respir Crit Care Med. 2010;181:734–42.
31. Mavragani CP, Nezos A, Moutsopoulos HM. New advances in the classification, pathogenesis and treatment of Sjogren's syndrome. Curr Opin Rheumatol. 2013;25:623–9.
32. Yao G, Qi J, Liang J, Shi B, Chen W, Li W, et al. Mesenchymal stem cell transplantation alleviates experimental Sjögren's syndrome through IFN-β/IL-27 signaling axis. Theranostics. 2019;9:8253–65.
33. Hu H, Dong L, Bu Z, Shen Y, Luo J, Zhang H, Zhao S, Lv F, Liu Z. MiR-23a-3p-abundant small extracellular vesicles released from gelma/nanoclay hydrogel for cartilage regeneration. J Extracell Vesicles. 2020;9:1778883.
34. Liu H, Zhang M, Shi M, Zhang T, Lu W, Yang S, Cui Q, Li Z. Adipose-derived mesenchymal stromal cell-derived exosomes promote tendon healing by activating both SMAD1/5/9 and SMAD2/3. Stem

Cell Res Ther. 2021;12:338.
35. Xu J, Wang D, Liu D, Fan Z, Zhang H, Liu O, et al. Allogeneic mesenchymal stem cell treatment alleviates experimental and clinical Sjögren syndrome. Blood. 2012;120:3142–51.
36. Tosolini M, Kirilovsky A, Mlecnik B, Fredriksen T, Mauger S, Bindea G, et al. Clinical impact of different classes of infiltrating T cytotoxic and helper cells (Th1, Th2, Treg, Th17) in patients with colorectal cancer. Cancer Res. 2011;71:1263–71.
37. Hwang SH, Park JS, Yang S, Jung KA, Choi J, Kwok SK, Park SH, Cho ML. Metabolic abnormalities exacerbate Sjögren's syndrome by and is associated with increased the population of interleukin-17-producing cells in NOD/ShiLtJ mice. J Transl Med. 2020;18:186.
38. Xiao F, Lin X, Tian J, Wang X, Chen Q, Rui K, et al. Proteasome inhibition suppresses Th17 cell generation and ameliorates autoimmune development in experimental Sjögren's syndrome. Cell Mol Immunol. 2017;14:924–34.
39. Lin X, Rui K, Deng J, Tian J, Wang X, Wang S, et al. Th17 cells play a critical role in the development of experimental Sjögren's syndrome. Ann Rheum Dis. 2015;74:1302–10.
40. Willis GR, Fernandez-Gonzalez A, Anastas J, Vitali SH, Liu X, Ericsson M, Kwong A, Mitsialis SA, Kourembanas S. Mesenchymal stromal cell exosomes ameliorate experimental bronchopulmonary dysplasia and restore lung function through macrophage immunomodulation. Am J Respir Crit Care Med. 2018;197:104–16.
41. Kim S, Lee SK, Kim H, Kim TM. Exosomes secreted from induced pluripotent stem cell-derived mesenchymal stem cells accelerate skin cell proliferation. Int J Mol Sci. 2018;19:3119.
42. Ozata DM, Gainetdinov I, Zoch A, O'Carroll D, Zamore PD. PIWI-interacting RNAs: small RNAs with big functions. Nat Rev Genet. 2019;20:89–108.
43. Chu H, Hui G, Yuan L, Shi D, Wang Y, Du M, et al. Identification of novel piRNAs in bladder cancer. Cancer Lett. 2015;356:561–7.
44. Mei Y, Wang Y, Kumari P, Shetty AC, Clark D, Gable T, et al. A piRNA-like small RNA interacts with and modulates p-ERM proteins in human somatic cells. Nat Commun. 2015;6:7316.
45. Yang J, Ling Y, Hua D, Zhao C, Sun X, Cai X, Chen J, Hu C, Cao P. IL-6R blockade by chikusetsusaponin IVa butyl ester inhibits Th17 cell differentiation and ameliorates collagen-induced arthritis. Cell Mol Immunol. 2021;18:1584–6.
46. Zheng Y, Dong C, Yang J, Jin Y, Zheng W, Zhou Q, et al. Exosomal microRNA-155-5p from PDLSCs regulated Th17/Treg balance by targeting sirtuin-1 in chronic periodontitis. J Cell Physiol. 2019;234:20662–74.
47. Li D, Kong C, Tsun A, Chen C, Song H, Shi G, Pan W, Dai D, Shen N, Li B. MiR-125a-5p decreases the sensitivity of Treg cells toward IL-6-mediated conversion by inhibiting IL-6R and STAT3 expression. Sci Rep. 2015;5:14615.

Table

Due to technical limitations, table 1 is only available as a download in the Supplemental Files section.

Figures

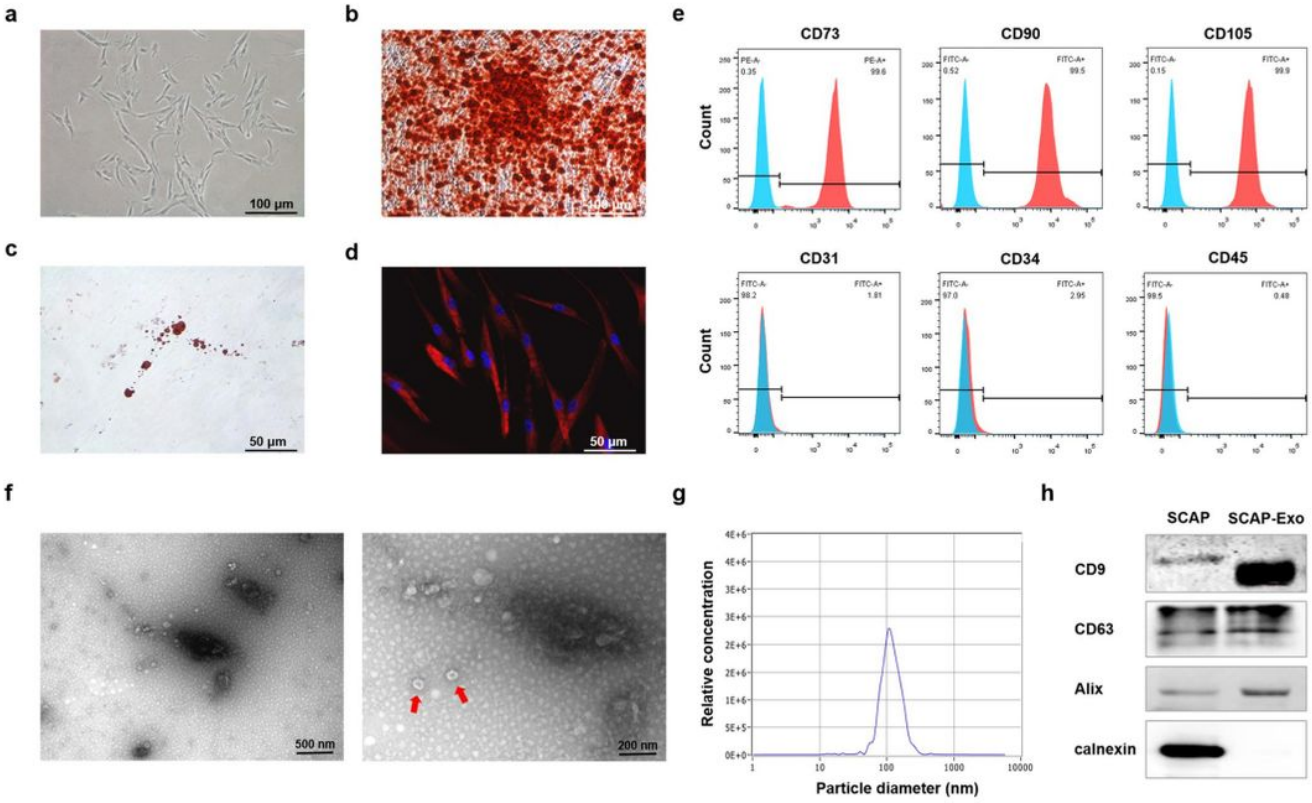

Figure 1

Characterization of SCAP and SCAP-Exo. a SCAP exhibited spindle-shaped morphology under a microscope. Scale bar = 100 μm. b Alizarin red S staining showed that SCAP formed mineralized nodes after osteogenic induction. Scale bar = 100 μm. c Oil red O staining showed that SCAP formed oil droplets after adipogenic induction. Scale bar = 50 μm. d Positive staining for the neurogenic marker βIII-tubulin in SCAP was observed after neurogenic induction. Scale bar = 50 μm. e SCAP was positive for the mesenchymal markers CD73, CD90 and CD105 and negative for the haematopoietic lineage markers CD31, CD34, and CD45. f TEM showed that the exosomes had a typical round or cup-shaped morphology. Scale bar = 500 or 200 μm. g NTA identified that the diameter distribution of these particles ranged from 30 to 150 nm with a mean of 113 nm. h Western blotting confirmed that SCAP-Exo had immunoreactivity for exosomal-specific antibodies against CD9, CD63, and Alix but not calnexin.

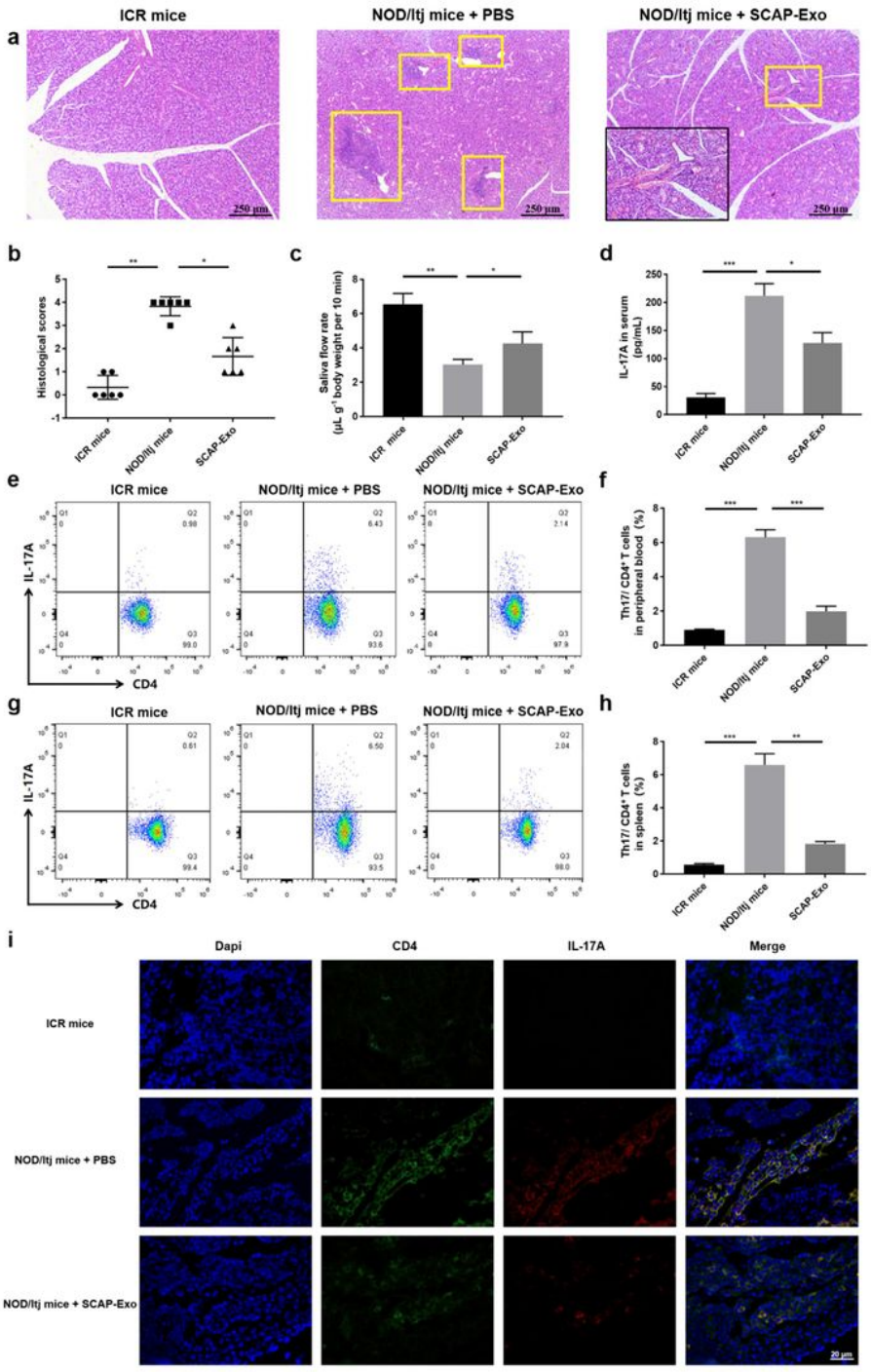

Figure 2

SCAP-Exo transplantation ameliorated SS mouse symptoms by downregulating Th17 cells. a H&E staining showed that there was almost no lymphocyte infiltration in the submandibular glands of healthy ICR mice; however, obvious masses of infiltrating lymphocytes were observed in the submandibular glands of NOD/ltj mice treated with PBS. NOD/ltj mice treated with SCAP-Exo had less lymphocytic infiltration and glandular atrophy than those treated with PBS. Scale bar = 250 μm. The yellow box

indicated the infiltrating lymphocytes. b Treatment with SCAP-Exo led to lower histological scores in the submandibular glands of NOD/ltj mice. c Measurement of saliva flow rate in mice showed that the saliva flow rate was increased in the SCAP-Exo transplantation group compared with that in the PBS transplantation group. d ELISA analysis showed that compared with PBS infusion, SCAP-Exo transplantation was associated with significantly lower IL-17A levels. e-f Flow cytometric analysis showed that SCAP-Exo transplantation exhibited a stronger capacity to downregulate the proportion of Th17/CD4+ T cells in the peripheral blood than PBS infusion. g-h Flow cytometric analysis showed that SCAP-Exo transplantation downregulated the proportion of Th17/CD4+ T cells in the spleen compared to PBS infusion. i Immunofluorescence staining showed CD4- and IL-17A-positive cells in the submandibular glands of mice. Scale bar = 20 μm. n = 6 in each group. *P < 0.05, **P < 0.01, ***P < 0.001. Error bars: mean ± SD.

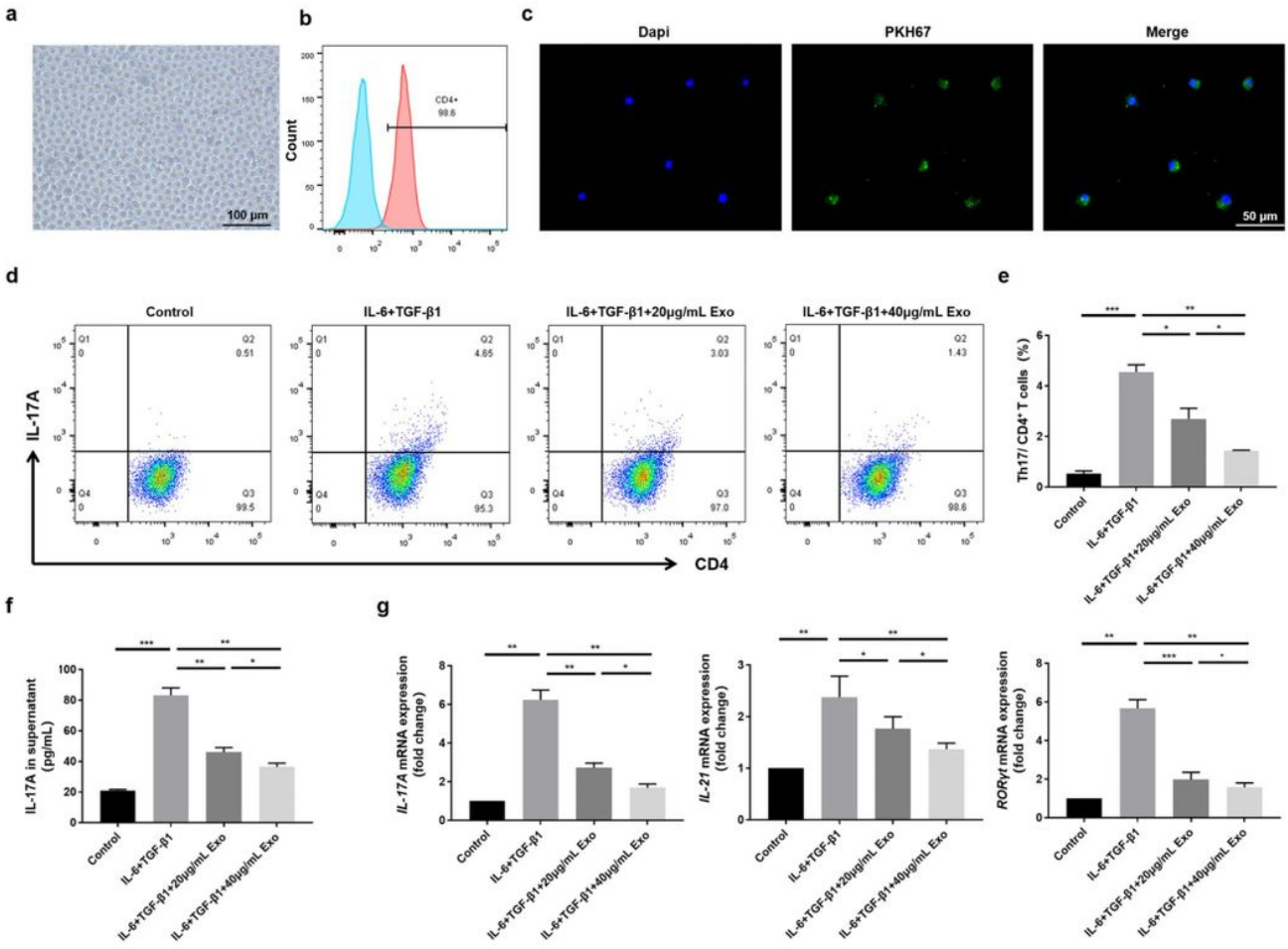

Figure 3

SCAP-Exo inhibited the differentiation of CD4+ T cells to Th17 cells. a Microscopic observation indicated that CD4+ T cells were round in the culture medium. Scale bar = 100 μm. b Flow cytometry showed that

the purity of CD4+ T cells was more than 90%. c Immunofluorescence staining showed PKH67 labelled SCAP-Exo (green) endocytosed by CD4+ T cells (counterstaining with DAPI; blue). Scale bar = 50 μm. d-e Flow cytometric analysis showed that the proportion of Th17/CD4+ T cells was downregulated by treatment with SCAP-Exo. f ELISA showed that treatment with SCAP-Exo reduced the IL-17A level in the supernatant. g RT-qPCR results showed that the mRNA expression levels of IL-17A, IL-21 and RORγt in CD4+ T cells were downregulated by treatment with SCAP-Exo. GAPDH served as an internal control. n = 3 in each group. *P < 0.05, **P < 0.01, ***P < 0.001. Error bars: mean ± SD.

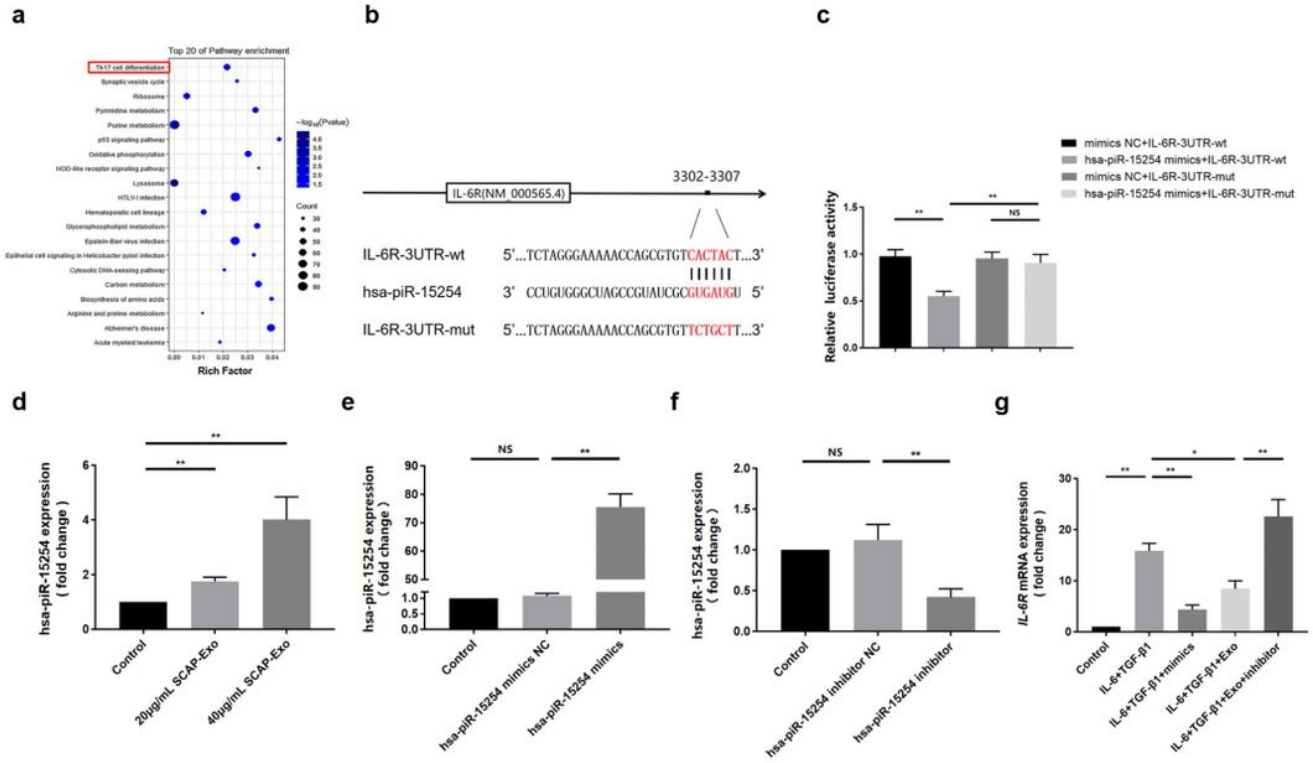

Figure 4

IL-6R mRNA was a direct target of hsa-piR-15254. a KEGG pathway enrichment analysis for the target genes of the top 40 piRNAs expressed in SCAP-Exo. The X-axis shows the percentage of the total number of annotated target genes in each pathway, and the Y-axis shows the pathway names. b Sequences of the predicted hsa-piR-15254 target sequences in the 3'UTR of IL-6R mRNA and its mutant containing nucleotide substitutions in the 3'UTR. c Luciferase reporter assays were conducted to test whether the IL-6R 3'UTR contains a binding site for hsa-piR-15254. Luciferase assays showed decreased reporter activity after cotransfection of the wild-type IL-6R 3'UTR plasmid with hsa-piR-15254 into 293T cells. d RT-qPCR revealed that after coculture with SCAP-Exo, the expression of hsa-piR-15254 in CD4+ T cells was significantly increased. e Hsa-piR-15254 mimics overexpressed the expression level of hsa-piR-15254 in CD4+ T cells. f Hsa-piR-15254 inhibitor downregulated the expression level of hsa-piR-15254 in CD4+ T cells. g The mRNA level of IL-6R was diminished in SCAP-Exo-treated CD4+ T cells and hsa-piR-

15254-overexpressing CD4+ T cells, whereas in the hsa-piR-15254 inhibitor group, the mRNA level of IL-6R was upregulated. n = 3 in each group. NS: P > 0.05. *P < 0.05, **P < 0.01. Error bars: mean ± SD.

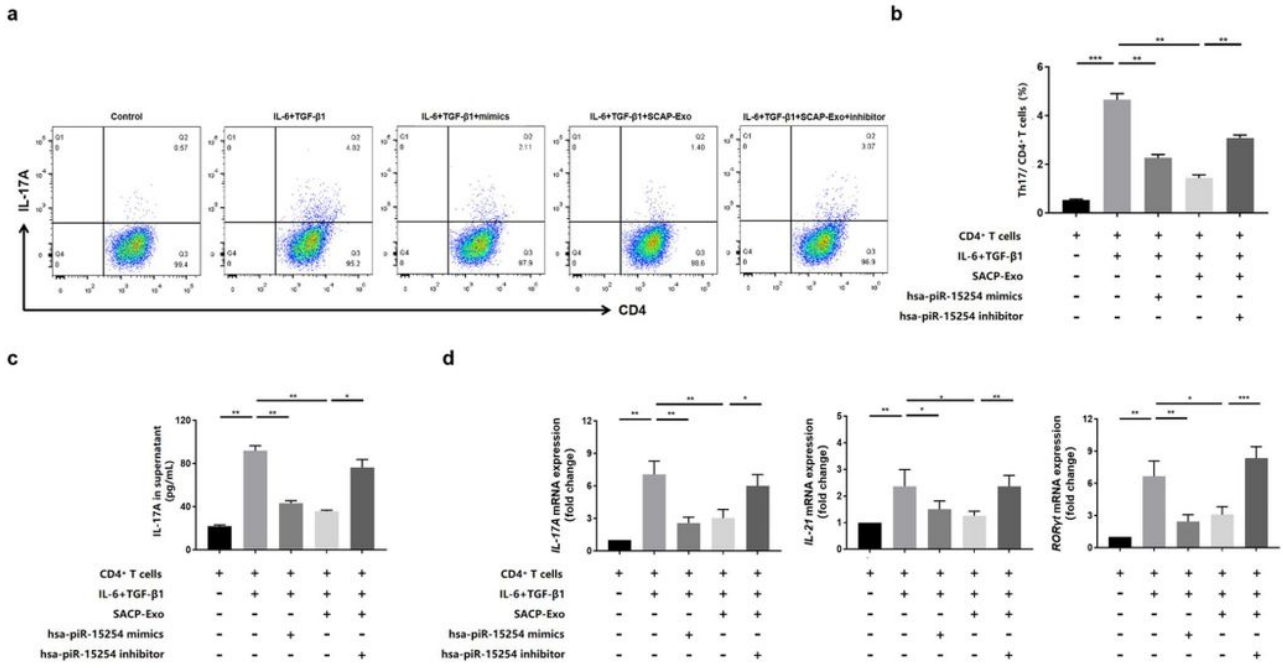

Figure 5

SCAP-Exo inhibited the differentiation of CD4+ T cells to Th17 cells through hsa-piR-15254. a-b Flow cytometry analysis showed that overexpression of hsa-piR-15254 downregulated the proportion of Th17/CD4+ T cells, whereas hsa-piR-15254 inhibition enhanced this proportion. c The IL-17A level in the supernatant was downregulated in the hsa-piR-15254 overexpression group and upregulated in the hsa-piR-15254 inhibitor group. d RT-qPCR results showed that the hsa-piR-15254 mimics suppressed the mRNA expression levels of IL-17A, IL-21 and RORγt in CD4+ T cells, whereas the expression levels of these genes were upregulated in the hsa-piR-15254 inhibitor group. GAPDH served as an internal control. n = 3 in each group. NS: P > 0.05. *P < 0.05, **P < 0.01, ***P < 0.001. Error bars: mean ± SD.

Supplementary Files

This is a list of supplementary files associated with this preprint. Click to download.

- AdditionalFile1.pdf
- Table1.pdf